Seasonal Changes in NDVI in Relation to Phenological Phases, LAI and PAI of Beech Forests

VERONIKA LUKASOVÁ *[a], MAIT LANG [bc] AND JAROSLAV ŠKVARENINA [a]

*[a] *Department of Natural Environment, Faculty of Forestry, Technical University in Zvolen, T.G. Masaryka 24, Zvolen 96053, Slovakia, veronika.brandysova@gmail.com, 00421455206210*

[b] *Department of Forest Management, Institute of Forestry and Rural Engineering, Estonian University of Life Sciences, Kreutzwaldi 5, Tartu 51014, Estonia*

[c]*Tartu Observatory, Tõravere, Tartumaa 61602, Estonia*

Lukasová, V., Lang, M. and Škvarenina, J. 2014. Seasonal Changes in NDVI in Relation to Phenological Phases, LAI and PAI of Beech Forests. *Baltic Forestry* 20(2): 248–262.

Abstract

The onset of the phenological phases, such as budburst, leaf development, flowering, fruiting, and leaf senescence, is evoked by the genetically determined internal periodicity of vegetation and significantly affected by climate conditions. Therefore, the timing of the onset of phenological phases is considered as a good indicator of climate change impacts. The phenological phases of ecosystems can be observed from satellites using the change in spectral radiance that is mainly driven by leaf optical properties, leaf arrangement and total leaf area in canopy.

In this study we used Normalized Difference Vegetation Index (NDVI) as an indicator of beech forests (*Fagus sylvatica* L.) seasonal dynamics in five test sites in Slovakia. During one growing season we analysed the phenological phases at each test site using three different approaches: i) *in situ* phenological observations, ii) digital hemispherical images taken to characterize the changes in the leaf area index (LAI) and in the plant area index (PAI), iii) NDVI calculated from space-borne MODIS sensor data. The estimates of LAI and PAI directly depend on the precision of canopy gap fraction (transmittance) estimates derived from the hemispherical images. Hence, we tested pixel classification based on the subjective decision of an operator and a recently proposed linear conversion of camera raw data (LinearRatio) which has been shown to produce comparable results to commonly used plant canopy analyzers.

The results showed that NDVI values reacted sensitively to the changes of vegetative phenological phases. The most rapid increase of NDVI was recorded during the leaf unfolding phenophase. After reaching its maximum, the NDVI values in all test sites started to decrease slowly during the summer. This was followed by the rapid decrease during leaf senescence in the autumn. The main changes in NDVI were well explained by the changes in LAI; however, the impact of LAI estimation method was significant. The canopy transmittance calculated from subjectively classified hemispherical images started to increase already in May, whereas the LinearRatio-based gap fraction continued to decrease until the end of July, which was in concordance with the observation performed *in situ*. The LAI estimates using canopy gap fraction from LinearRatio procedure did not indicate the saturating relationship with NDVI at high LAI values (LAI > 3) as reported by many authors. According to our results, MODIS NDVI can be used to observe phenological phases in mature beech forests. For the calculation of transmittance, which is required to estimate leaf area index from hemispherical images, we recommend using LinearRatio based methods.

Key words: beech, NDVI, LAI, PAI, phenological phases

Introduction

The changes in the onset of phenological phases recorded in long-term observations are considered as a suitable indicator of climate change (Menzel 2002, Chmielewsky and Rötzer 2001). Changes in the timing of plant developmental phases those are caused by the current (anthropogenic) global climate change can significantly affect ecosystem productivity, competition between plant species, and interaction with heterotrophic organisms (Badeck et al. 2004). Phenological phases such as leaf onset, flowering, fruiting and leaf senescence have been visually observed and documented for a long time (Sparks and Carey 1995, Menzel 2000, Čufar et al. 2012). During the recent decades new methods have been developed those use satellite remote sensing data, conventional digital photos or hemispherical digital photographs for phenological observations (Zhang et al. 2003, Fisher and Mustard 2007, Ganguly et al. 2010, Jönsson et al. 2010, Guyon et al. 2011).

Spectral properties of plant canopies are determined mainly by photosynthesis, canopy structure and visible background (Liang 2004, Kuusk and Nilson 2000). Modern sensors are capable of recording spectral radiance in narrow spectral bands (wavelength

intervals) and can provide high resolution spectral signatures for plant canopies. In remote sensing, there are some simple spectral indices that have been used for monitoring green plant communities. Tucker (1979) showed that radiance in the red and near-infrared spectral region can be combined into a multispectral index, which has strong relationship with the amount of the photosynthetically active green biomass – usually leaves or needles, in plant canopies. Since then, the Normalized Difference Vegetation Index (NDVI) has been widely used in many remote sensing applications including phenology studies (Beck et al. 2006, Soudani et al. 2008, Narasihman and Stow 2010, Jeong et al. 2011, Brandýsová and Bucha 2012). New modifications of the NDVI are EVI – Enhanced Vegetation Index (Zhang et al. 2003, Ganguly et al. 2010), PVI – Perpendicular Vegetation Index (Guyon et al. 2011) and WDRVI – Wide Dynamic Range Vegetation Index (Jönsson et al. 2010). However, the new versions of NDVI include additional spectral bands and may also require additional parameter values to be estimated by the user. This is a major drawback when are multispectral indices that assessing small patches in landscape because the spatial resolution of the additional bands is usually lower. For example, the EVI index includes blue spectral channel, which has much coarser spatial resolution in the widely used global monitoring space-borne MODIS data (Heinsch et al. 2003).

Several types of phenology metrics can be derived from remote sensing data. Numerically the value of such a metric gives usually day of the year of the occurrence of the phenomena. Liang et al. (2011) used NDVI time series curvature change *K'* published by Zhang et al. (2003) to identify green-up, maturity, senescence and dormancy. TIMESAT software (Jönsson and Eklundh, 2002, 2004; Eklundh and Jönsson, 2011) allows to calculate the start of season and end of season. Lange and Doktor (2013) have released phenex package for R statistical software to calculate green-up, season maximum and senescence.

The foliage of plants is the most changing structural element of forests during growing period. To assess the amount of leaves, Watson (1947) defined dimensionless leaf area index (LAI) as the total one-sided area of photosynthetic tissue of flat leaves per unit ground area. LAI is a key structural characteristic of forest ecosystems because of the role of green leaves in controlling many biological and physical processes in plant canopies. A comprehensive overview about LAI measurement and estimation methods is given by Jonckheere et al. (2004). One of the popular LAI estimation methods is based on the hemispherical images. First, the amount of open sky has to be estimated. Then, LAI can be calculated from the angular distribution of canopy transparency (gap fraction). Since the era of the photographic film, a method called thresholding (binary classification) has been used to separate sky and plant pixels. However, the selection of optimal threshold between sky and forest canopy has remained a challenge without a final solution for over decades in a human operator based methods or automated algorithms (Jonckheere et al. 2005). There is a wide variety of different well-known automatic and operator-dependent thresholding techniques and software for canopy analyses: WinSCANOPY (Regent Instruments Inc. © 2013), SOLARCALC (Chazdon and Field 1987), Winphot (Ter Steege 1997), CIMES (Walter 2009), CanEye (Baret and Weiss 2010). As a new approach, Cescatti (2007) showed how to use modern digital cameras similarly to plant canopy analyzers and proposed LinearRatio method. The correct transmittance measurement is just the first step: sophisticated models and auxiliary data about canopy structure are needed to obtain the true green leaf area index for a forest (Nilson and Kuusk 2004). However, most of the hemispherical image processing software packages calculate plant area index (PAI) instead of LAI. In addition, digital hemispherical photography poses specific problems when deriving LAI over sloping terrain (España et al. 2008).

In this study, we focused on the applicability of NDVI derived from 250 m resolution space-borne MODIS images to observe phenology-driven seasonal changes, in five mature beech forests located near Zvolen, Slovakia. We calculated the seasonal NDVI course using the MODIS red and near infrared spectral bands performed *in situ* phenology observations and took below-canopy upward looking hemispherical images. The true green LAI (LAI_{LR}) was obtained from the inversion of the model published by Nilson and Kuusk (2004) that used canopy transmittance based on LinearRatio method. The CanEye program was used to calculate the effective plant area index (PAI_{CE}). We assumed that both canopy LAI_{LR} and PAI_{CE} have similar relationship with NDVI and that there are no differences in their seasonal courses. We analysed the occurrence of the observed phenophases in relation to NDVI and LAI estimations. For each stand we calculated phenology metrics based on NDVI time series by using *K',* TIMESAT and phenex. The metrics were assessed by using *in situ* observations.

Material and Methods

Study sites

The study sites were located on the territory of the University Forest Enterprise belonging to the Technical University in Zvolen, situated in central

Slovakia at localities of Turova (48°38'N; 19°03'E) and Bukovina (48°34'N; 19°02'E).

The forest management plan database and Landsat TM images based on tree species composition map of the Slovak forests (Bucha 1999) were used to select the test stands. The area of one forest unit in Slovak forests is usually 15–20 hectares and contains 2 or 3 MODIS pixels. However the species composition from the forest management plan represents whole forest unit and does not include the information of spatial distribution of tree species in the unit, the Landsat TM 30 m data were used to identify the parts of forest unit, where the beech is most dominant tree species. The species composition map was aggregated from 30 m to 250 m pixels corresponding to MODIS red and near-infrared images. The 250 m pixels with more than 60 % of beech were classified as a "beech" class. The pixels on the boundary between beech forests and other land cover classes or forest types were excluded due to possible spectral contamination. This follows from the shape of the instrument point spread function and positional accuracy of the MODIS image localization, which is ~ 50 m at nadir (Wolfe et al. 2002). We selected pixels in five relatively homogenous forest units (stands) dominated by *Fagus sylvatica* and with minimal presence of conifers. The stands were sufficiently large regarding the 250 m (6.25 ha) spatial resolution of the MODIS images (Justice et al. 2002). The vertical structure of the stands was differentiated containing rich undergrowth layer of *Fagus sylvatica* with the admixture of *Carpinus betulus* (L.). The basic characteristics of the test stands are given in Table 1.

Calculation of the seasonal NDVI from the MODIS data

Daily red and near-infrared spectral images from the Moderate Resolution Imaging Spectroradiometer (MODIS) onboard Terra and Aqua satellites were used to calculate the seasonal course of NDVI for each test stand. For our purpose, the suitable product was MOD09GQ, a daily surface reflectance. The MOD09GQ contains red spectral band (RED 620–670 nm) and near infrared spectral band (NIR 841–876 nm) with 250 m spatial resolution. The NDVI product from MODIS data processing system was not used, since it represents an average NDVI for the 16 day period, which is not suitable to detect fine changes in phenology. We also disregarded EVI index because it includes the blue band of coarser spatial resolution (500 m). The MODIS images were projected into the Slovak civil coordinate system (S-JTSK). We also downloaded the quality control data (MOD09GA) to check the recorded reflectance at pixel level in each individual image for possible clouds, fogs aerosols etc. according to the flags in the quality control data (Vermote et al. 2011). The image pixels, which did not match the quality criteria in the quality analysis, were eliminated from further analyses.

Based on the MOD09GQ product we calculated NDVI, which is considered as a biophysical indicator of the phenological phases

$$NDVI = \frac{NIR - RED}{NIR + RED} \quad (1)$$

Table 1. The basic characteristics of forest test stands

Stand	509	514	531	541	619
Altitude (m a.s.l.)	447	560	591	602	532
Slope (°)	14	22	22	22	17
Aspect	W	W	W	E	N
Species composition of canopy (%)	FS 90 QP 5 PS 5	FS 80 QP 10 AA 10	FS 85 QP 10 AA 5	FS 100	FS 80 QP 20
Species composition of undergrowth (%)	FS 90 CB 10	FS 95 CB 5	FS 80 CB 20	FS 100	FS 95 CB 5
Stocking level	0.9	0.8	0.8	0.9	0.9
Canopy cover	0.9	0.9	0.9	0.9	0.9
Age (years)	58	103	73	83	68
Canopy trunk diameter (cm)	21	34	22	30	24
Undergrowth trunk diameter (cm)	8	11	9	13	10
Canopy height (m)	19	25	22	28	25
Undergrowth height (m)	12	12	10	12	13
Number of canopy trees (trees / m^2)	0.076	0.045	0.076	0.038	0.045
Number of undergrowth trees (trees / m^2)	0.102	0.054	0.080	0.041	0.032

FS *is Fagus sylvatica* L., QP *is Quercus petrea* L., PS *is Pinus sylvestris* L., CB *is Carpinus betulus* L., AA *is Abies alba* L.

For each stand we obtained 58 NDVI values for the vegetation period of the year of 2011. In case of the missing NDVI values on the dates corresponding to *in situ* phenological observations, the value of NDVI was interpolated from the nearest previous and the next day with the NDVI value.

Hemispherical images

The hemispherical images were taken to measure the angular distribution of the canopy gap fraction and to estimate the leaf area index and plant area index. In each stand a regular sampling grid of nine marked sampling points was established. The distance between two neighbouring points was 50 meters (Figure 1). Seven measurements were carried out at each point during the growing season of 2011: 3–4 May (further in the text referred as day of year: DOY 123), 12–13 May (DOY 133), 19 June (DOY 170), 10–11 August (DOY 222), 28–29 September (DOY 272), 17–18 October (DOY 290), and 15–21 November (DOY 319). One hemispherical image was acquired at one meter height from the ground on each selected day of year. After the measurement of the nine points, dark image frames with the lens cover on were also taken. The final dataset contained 315 hemispherical images of the forest canopy that were collected during the vegetation period from May to November. Due to the technical reasons the imaging was not possible before May.

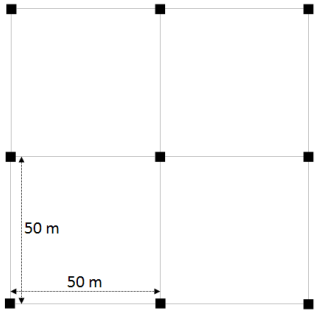

Figure 1. Sampling grid established in each of five beech stands. ■ – sampling point for taking hemispherical image

The first four measurements were carried out with a Nikon camera and after it had broken down, a Canon camera was used for the next three measurements (Table 2). The images were taken under the conditions with close to diffuse skylight – during sunrise and sunset, or during cloudy and partially cloudy days. The cameras were operated in the standard pre-programmed mode (P-mode), which adjusts the aperture and the shutter speed automatically. These cameras were set to store image data in the raw format (no processing in camera). This retained the linear relationship between the incident light and pixel values, and the data corresponded to the plant canopy analyzer LAI-2000 measurements as proven by Cescatti (2007).

Table 2. The settings of the hemispherical cameras

Camera type	Nikon Coolpix E5400	Canon EOS 450D
Used on DOY	123, 133, 170, 222	272, 290, 319
Imaging mode	P - Programmable automatic program	P is Programmable automatic program
Aperture	Adjusted by camera	Adjusted by camera
Shutter speed	Adjusted by camera	Adjusted by camera
Lens	Fisheye converter FC-E9	Sigma 4.5mm F2.8 EX DC HSM
Sensor size	2592 × 1944	5184 × 3456
ISO	100	200
Metering mode	Centre weighted average	Spot

The radiance data were extracted from the raw file of the hemispherical camera with *dcraw* (Coffin 2011) free utility and dark image frames were subtracted. Only the pixels with the original blue filter according to the camera sensor filter pattern were used in the further analysis.

Two methods were used to calculate the canopy gap fraction and to estimate canopy structural indices (LAI and PAI). The first gap fraction calculation method is described in Lang et al. (2010), who adjusted LinearRatio (Cescatti 2007) for a single camera. According to Cescatti (2007) the canopy gap fraction is a ratio between the below canopy image and the above canopy image. In this study, the above canopy reference was not measured but created for each below canopy image similarly to Lang et al. (2010) by combining the interpolation of the canopy gap pixel values and a sky radiance model (Bartzokas et al. 2003). More than 20 open sky points were marked for each image. 3 × 3 pixel windows were used around each mark to calculate the incident radiation of clear sky. The ratio of the below canopy image (I_B) to the above-canopy (I_A) image was used to calculate canopy transmittance $T = I_B / I_A$ from each image. The average transmittance for each stand and for each field observation date was calculated from the nine transmittance images. A slope mask for each stand was created and applied to the transmittance image. Since the cameras were not calibrated in the lab, vignetting correction and projection correction were not applied. We assumed a linear projection model for both cameras. The small errors in the projection model do not have a significant influence in our analysis. The vignetting effects were to some extent eliminated by the nature of the LinearRatio method.

The second method for gap fraction estimation was based on the subjective classification of pixels and was carried out in CanEye software. The dark current corrected images were converted into the compressed .jpg format using 5% saturation criteria at both ends

of the pixel value distribution histogram. These images are further referred as FE.jpg images. The saturation criterion was needed to retain the most informative part of pixel values after the data conversion from 16 bit to 8-bit, since CanEye works only with 8-bit data.

The estimation of LAI_{LR} by inverting gap fraction model

The canopy transmittance obtained from Linear Ratio method was used to invert the gap fraction model (Nilson 1999, Nilson and Kuusk 2004) in order to estimate the true green leaf area index LAI_{LR} for each observation day and stand as follows:

$$LAI_{LR} = \frac{-2N}{\kappa + \alpha} \int_0^{\frac{\pi}{2}} S(\theta) \ln \left[1 - \frac{1 - exp\left[\frac{(1-\xi)\ln a(\theta)}{NS(\theta)} \right]}{1-\xi} \right] \cos\theta \sin\theta d\theta \quad (2)$$

where N is the stand density (trees/m^2), κ is shoot-level clumping factor, α is the branch area to leaf area ratio, $S(\theta)$ is crown envelope projection area (m^2) on the horizontal plane in the direction of view zenith angle θ, ξ is Fisher's grouping index of the tree distribution pattern, $a(\theta)$ is the measured fraction canopy gaps at the view angle θ from LinearRatio method. To apply Eq. (2), estimates of N, κ, α, as well as tree dimensions – crown length L_{CR}, crown radius R_{CR}, tree height h and trunk diameter at breast-height $D_{1.3}$ should be known. N was calculated from *in situ* tree counts within 3 circular sample plots with 20 m diameter. Shoot-level clumping index κ is equal to 1 for randomly distributed foliage, > 1 for regularly distributed foliage, and < 1 for clumped canopies (Weiss et al. 2004). For observed beech stands κ was set to 0.8. Two possible crown forms can be used in the Nilson and Kuusk (2004) model: an ellipsoid for deciduous species and a cone on the top of a cylinder for conifers (Kodar et al. 2008). We used the ellipsoid as a crown form for beech. The branch area ratio was estimated according to percent coverage of leafless trees from digital images, which were processed using object-oriented segment-based classification. Fisher's grouping index was calculated from the relation

$$\xi = -\ln(1 - C_{CAN}) / C_{CR} \quad (3)$$

where C_{CAN} is the canopy cover in midsummer (sum of the vertical crown projection areas per unit ground area, overlapped areas counted only once, see Jennings et al. (1999) for definitions) estimated from the gap fraction data using zenith annuli $0° \le \theta \le 15°$. C_{CR} is the crown cover (sum of the vertical crown projection areas per unit ground area) calculated as $C_{CR} = N \cdot R_{CR}$ according to the stand density (N) and crown radius (R_{CR}) (Kodar et al. 2008).

The estimation of plant area index using CanEye

Canopy transmittance estimation in CanEye software is based on the subjective classification of image pixels as "open sky" and "plant element" classes. For forests the output from CanEye is the effective plant area index (PAI_{CE}) since the influence of trunks and branches is not eliminated. The following parameters were defined to run the program: calibration parameters (image size, optical center, projection function and circle of interest, sub-sampling factor) and angular resolution (azimuth, zenith). First order polynomial $D_f = 90° / R_{90}$ was used as the projection function relating the distance from image center to the actual view zenith angle. For the Nikon camera, the value of the projection model was $D_{f,nikon} = 0.1125$ and for the Canon it was $D_{f,canon} = 0.06494$. The slope mask was used to exclude the ground area captured on images. To minimize the effect of operators' subjectivity, the classification was repeated four times and the average effective plant area index PAI_{CE} was used for each stand and observation date.

In situ phenological observations

Visual phenological observations were carried out in the test stands during the whole vegetation period in 2011 using the method published by SHMU (1984). Following this method, ten mature beech trees (more than 50 years old) were selected in each stand to monitor the phenological phases described in Table 3. These trees should be representative – not early or late flushing in comparison with all other trees, and situated inside the forest at least 50 m from the forest edge. Each phenophase (except for FLU) has three basic states: beginning (10% onset), when 10% of the

Table 3. The observed phenological phases, their definitions and abbreviations (Abbr.)

Phenophases	Definition	State of phenophase	Abbr.
bud swelling (BS)	when buds extended their length and green appeared on edges of bud scales	10 %onset 50 %onset 100 %onset	BS_{10} BS_{50} BS_{100}
budburst (BB)	when bud scales opened and green top of leaf was sticking out	10 %onset 50 %onset 100 %onset	BB_{10} BB_{50} BB_{100}
leaf unfolding (LU)	when leaves had final shape, but not final size and colour	10 %onset 50 %onset 100 %onset	LU_{10} LU_{50} LU_{100}
final leaf unfolding (FLU)	when leaves had final size and colour	100 %onset	FLU_{100}
leaf colouring (LC)	when leaves changed their colour from green to yellow, red or brown	10 %onset 50 %onset 100 %onset	LC_{10} LC_{50} LC_{100}
leaf fall (LF)	when leaves fell down from trees to the ground	10 %onset 50 %onset 100 %onset	LF_{10} LF_{50} LF_{100}

trees have reached the phenophase; general (50 % onset), when 50 % of the trees have reached the phenophase; and full (100 % onset), when 100 % of the trees reached the phenophase.

Assessment of NDVI time series based phenology metrics

We used the NDVI time series curvature change method (Zhang et al. 2003) to estimate green-up, maturity, senescence and dormancy. The NDVI observations for each stand were pooled at DOY = 180 and then fitted with logistic model given in Zhang et al. (2003) by using the method in R. The phenology metrics were calculated from the fitted function curvature change *K'*.

For processing the single year data in TIMESAT, we had to replicate the data from the year of 2011 and to create a three-year long series according to instructions given by Eklundh and Jönsson (2011). NDVI data were fitted with logistic function (number of envelope iterations = 2) and with Savitzky-Golay adaptive filtering (number of envelope iterations = 1, window size = 3). The rest of the settings were similar for both methods. The relative NDVI level 0.1 was specified as the season start and the season end criterion for the phenology metrics calculation. TIMESAT calculates the DOY of the start of season and of the end of season, which were interpreted as green-up and dormancy.

The phenex package (Lange and Doktor 2013) is designed for calculation of phenology metrics from a single year NDVI data. For each day of the year a NDVI value is required. We used the NDVI = 0.4 for DOY = 1 and 10% decreased NDVI of the last observation for DOY = 365 and filled all gaps in the data series with the approx function in R (R Core Team 2012). All available data fitting methods in phenex procedure modelValues were tested by using default settings and the fitted values were then used in the phenoPhase method to calculate green-up, maximum and senescence metrics when local threshold was set to 0.1.

Results

The observed phenological phases in the study stands

During the growing season in the year of 2011 two main phenological events occurred in the test beech forests: leaf onset (during spring) when LAI_{LR}, PAI_{CE} and NDVI increased and leaf offset (during autumn) when LAI_{LR}, PAI_{CE} and NDVI decreased. The onset days of all observed phenophases and their developmental stages in the test stands are listed in Table 4.

Table 4. The onset days (DOY) of *in situ* observed phenological phases

Phenophase	Stand No.				
	509	514	531	541	619
BS_{10}	98	99	101	99	101
BS_{50}	101	101	104	102	105
BS_{100}	105	105	106	104	107
BB_{10}	106	106	107	105	108
BB_{50}	108	110	110	110	111
BB_{100}	111	113	112	112	113
LU_{10}	112	114	113	113	114
LU_{50}	115	118	117	116	117
LU_{100}	121	123	123	122	122
FLU	158	158	159	159	160
LC_{10}	267	269	262	273	278
LC_{50}	283	285	266	298	300
LC_{100}	300	306	303	304	306
LF_{10}	292	289	280	295	294
LF_{50}	306	306	303	304	306
LF_{100}	314	316	313	316	319

The estimates of canopy transmittance, LAI_{LR} and PAI_{CE}

The hemispherical images were acquired under the best possible diffuse illumination conditions, but some measurements were affected by the direct solar illumination (Table 5).

Table 5. The illumination conditions of the days when the hemispherical images were taken

Date	average DOY	Stand				
		509	514	531	541	619
May 3	123	W (3)	W	W	W	-
May 4		B (6)	-	-	-	SB
May 12	133	-	B	B	SL	-
May 13		L	-	-	-	L
Jun 19	170	L	W	L	L	L
August 10	222	-	-	L	L (6)	-
August 11		B	B	-	L (3)	W
September 28	272	-	L	-	W	W
September 29		W	-	W	-	-
October 17	290	-	L	L	W	-
October 18		W	-	-	-	W
November 15	319	-	L	-	L	-
November 16		L	-	L	-	-
November 21		-	-	-	-	G

Legend: illumination conditions (colour of the sky): S is crowns illuminated by sun/incidence of sun, L is light blue sky, B is blue sky/partially cloudy sky, W is white sky, G is grey sky. The number in brackets is the number of canopy images taken on the particular day if differed from nine.

The LinearRatio method accounts for the differences in the sky radiation since the above canopy image is created using the information from the below canopy image. However, compared to the subjective classification in CanEye program LinearRatio method seemed to be more sensitive to the direct sunlight and to the image exposure problems inherent in the pre-programmed P-mode that was used in the cameras. The

incidence of direct sunlight sometimes occurred during early mornings; and due to the illuminated trunks and leaves the transmittance estimates were positively biased. This increase in the gap fraction estimates resulted in lower LAI_{LR} values as shown in Figure 2d,e) in stands 541 – DOY 133 and 619 - DOY 123. The discrepancies were also found during early mornings, when the sky was clear and blue. Sometimes the camera automatic settings in P-mode imaging using the spot light metering mode were not set properly under dense canopies. This resulted in exceptionally small transmittance (gap fraction) values and fluctuating high LAI_{LR} values as shown in Figure 2a-c) in stands 509 – DOY 222, 514 – DOY 133 and 222, 531 – DOY 133. All these problematic LAI_{LR} values were excluded from further analyses.

The fluctuations of PAI_{CE} estimates during the vegetation period of 2011 were smaller than the fluctuations of LAI_{LR}. However, the seasonal course of the plant area index PAI_{CE} did not follow the observed phenological phases which, on the other hand, were in good concordance with the seasonal changes of LAI_{LR}. The LAI_{LR} rose until the midsummer and then started to decrease until the winter season. The behaviour of PAI_{CE} was different, since the decrease started already during May and lasted till June. From the end of June to August, PAI_{CE} did not change, and subsequent decrease was observed from September until December (Figure 2a-e). This probably resulted from the operator-driven classification (thresholding) used to estimate PAI_{CE}.

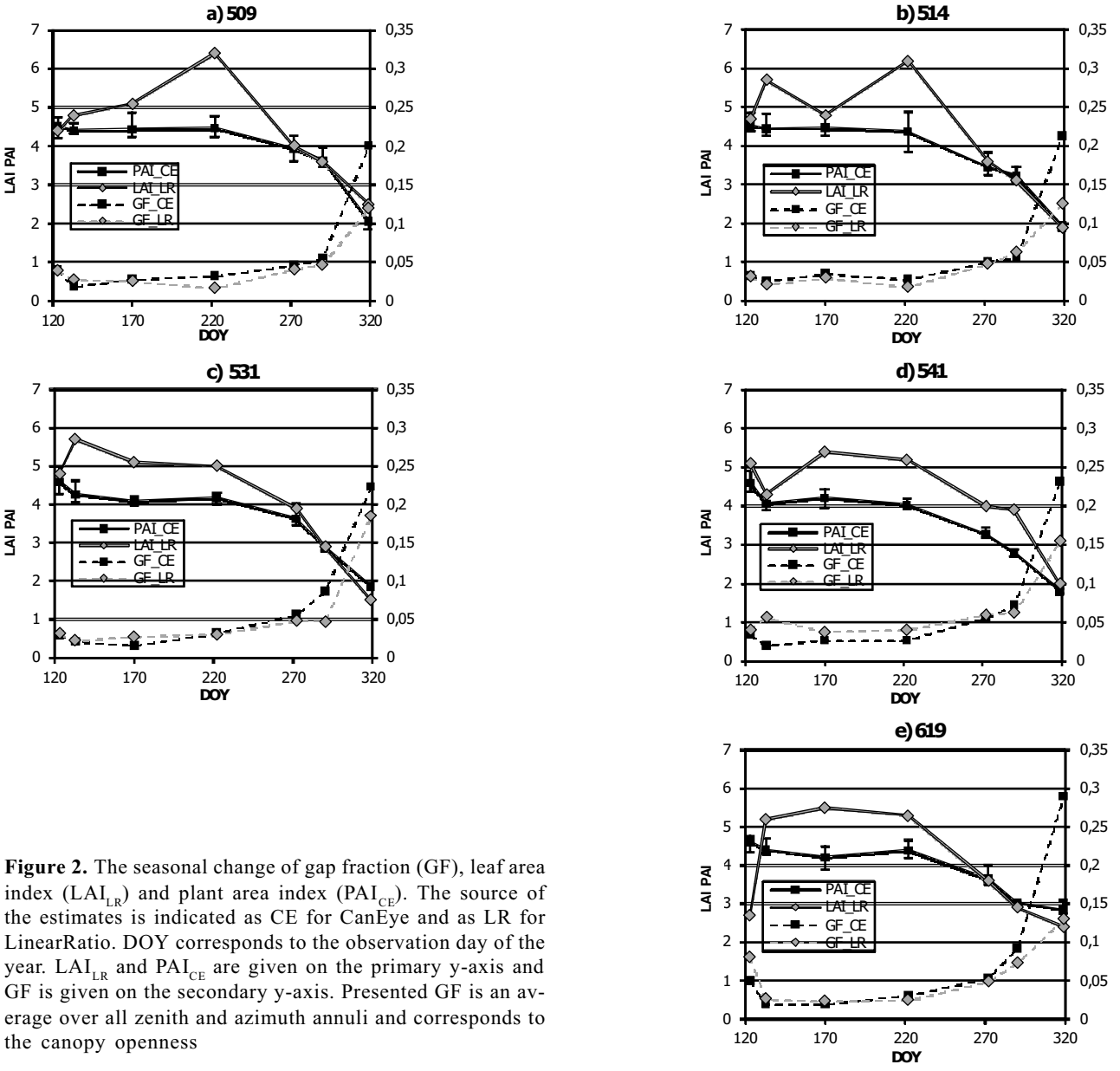

Figure 2. The seasonal change of gap fraction (GF), leaf area index (LAI_{LR}) and plant area index (PAI_{CE}). The source of the estimates is indicated as CE for CanEye and as LR for LinearRatio. DOY corresponds to the observation day of the year. LAI_{LR} and PAI_{CE} are given on the primary y-axis and GF is given on the secondary y-axis. Presented GF is an average over all zenith and azimuth annuli and corresponds to the canopy openness

After excluding the problematic LAI_{LR} values that resulted from bad camera settings or the direct incidence of the Sun, we applied the 4th order polynomial function to describe the LAI_{LR} and PAI_{CE} changes during the growing season (Figure 3). The relationship between the two independent canopy indices LAI_{LR} and PAI_{CE} was linear with the coefficient of determination $R^2 = 0.84$ (Figure 4). The intercept in LAI_{LR}-PAI_{CE} relationship was not 0 and represents branch area index BAI estimate ($PAI_{CE} - LAI_{LR} \approx BAI$).

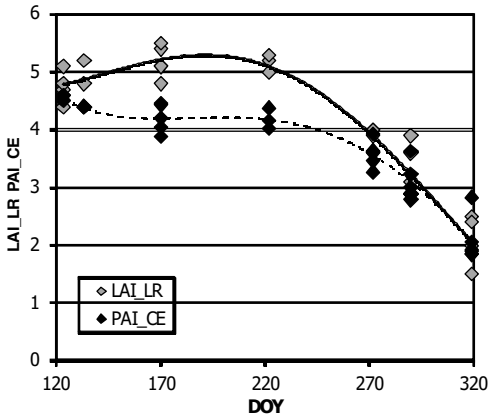

Figure 3. The seasonal course of LAI_{LR} and PAI_{CE} in the year 2011 fitted with 4th order polynomial function

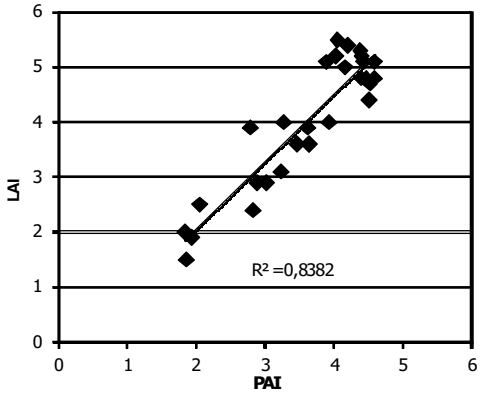

Figure 4. The relationship between the true green leaf area index LAI_{LR} and the plant area index PAI_{CE}

The relationships between NDVI, canopy indices and phenophases

The seasonal change of NDVI (Figure 5) and LAI_{LR} followed the main phenological phases. The bud swelling (BS) was the first vegetative phenological phase observed on beech. This phenophase started around DOY 100 when NDVI based on the satellite images was already increasing, although there were no green leaves in the tree canopy. This early increase in NDVI was probably caused by the forest understory vegetation.

The next phenophase of budburst, the BB_{10}, began around DOY 106. The NDVI recorded on this DOY was 0.56. The most rapid increase of NDVI from 0.58 to 0.87 (Figure 5) was recorded during the phenophase of leaf unfolding, LU (from DOY 112 to 123). Unfortunately, due to the technical reasons we could not start taking hemispherical images before the end of leaf unfolding and hence, we could not analyze the changes in canopy transmittance in this period. At the end of the spring phenophases, in the period from LU_{100} (DOY 123) to the phenophase FLU_{100} (DOY 159), a slight increase of NDVI from 0.87 ($s_x = 0.009$) to 0.92 ($s_x = 0.010$) and LAI_{LR} were still recorded. The maximum LAI_{LR} values were recorded during FLU_{100} phenophase (DOY 170). The differences in the onset of phenophases between the stands during the spring were small, with the average variation range of 3 days ($s_x = 1$ day).

After reaching the full leaf area, forest NDVI values started to decrease already in the summer, and in the middle of August (DOY 222) NDVI decreased to 0.9 ($s_x = 0.007$). Similar pattern was revealed also for LAI_{LR} values.

The autumn phenophases started at the end of September. The between-stand differences in NDVI values were larger in the autumn than in the spring. The earliest autumn reduction of NDVI was recorded in stand 531, where the phenological phase LC_{10} and LC_{50} occurred earlier than in other stands (Table 4). The latest onset of leaf colouring was observed in stand 619, where LC_{50} occurred on DOY 300. These differences disappeared after the first autumn rain and temperature drop, when all leaves became totally brown within few days (DOY 305). For a better imagination of the autumn phenological situation we present a comparison for DOY 290: in stand 531 NDVI = 0.74 during LC_{70} while in stand 619 NDVI = 0.79 was during LC_{30}. LAI_{LR} values decreased simultaneously with the drop of NDVI, although the phenophase LF_{10} started on DOY 290 on average ($s_x = 5.2$). The decrease in LAI_{LR} before the phenophase LF_{10} is probably caused by the violation of the assumption of black leaves (transmittance reflectance 0) in the optical measurements of the leaf area index estimation. In the blue spectral region, the absorption is mainly caused by chlorophyll. The leaf coloring indicates chlorophyll decay and an increase in leaf reflectance in the blue spectral region. As a result, the ratio between the below canopy and the above canopy radiances increases causing the underestimation of LAI (which is not green any more).

The timing patterns of the leaf fall were similar to the leaf colouring phenophases. The leaf fall (LF_{10}) in stand 531 started at the beginning of October (DOY 280), i.e. 9-15 days earlier than in the other stands. The phenological situation between LF_{50} and LF_{100} was

quite similar in all stands (Table 4). The phenophase LF_{50} started around DOY 304 and LF_{100} was observed around DOY 316. After LF_{100} and before the snow cover, NDVI decreased to the stable value, NDVI = 0.54 (s_x = 0.016), on average, and LAI_{LR} dropped to its minimal value.

The seasonal course of PAI_{CE} differed from the seasonal course of NDVI during the transition from the spring to the summer, as PAI_{CE} started to decrease already after LU_{100}. However, at that time NDVI still showed a slight increase. In the autumn, the seasonal courses of NDVI and PAI_{CE} were similar.

LAI_{LR} had strong linear relationship with NDVI described by the coefficient of determination, R^2 = 0.85 (Figure 6). Although LAI depends mainly on the amount of leaf biomass, while NDVI depends also on the colour of the leaves, both indices were rising during spring phenophases and were decreasing during autumn phenophases. In the spring, the enlarging of leaf area expressed by LAI_{LR} was coupled with the increasing of greenness captured by NDVI. In the summer after FLU_{100} both indices slightly decreased. In the autumn NDVI and LAI_{LR} simultaneously decreased. Although seasonal courses between PAI_{CE} and NDVI differed, the coefficient of determination expressing the linear relationship between these two indices was also high, R^2 = 0.82 (Figure 6). We discovered no significant difference between the coefficients of determination of LAI_{LR} to NDVI relationship and PAI_{CE} to NDVI relationship.

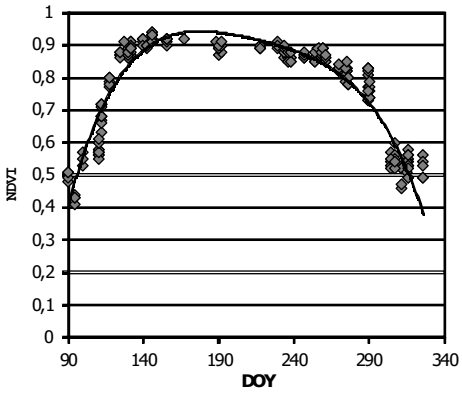

Figure 5. The seasonal course of NDVI during the year of 2011 fitted with 4th order polynomial function

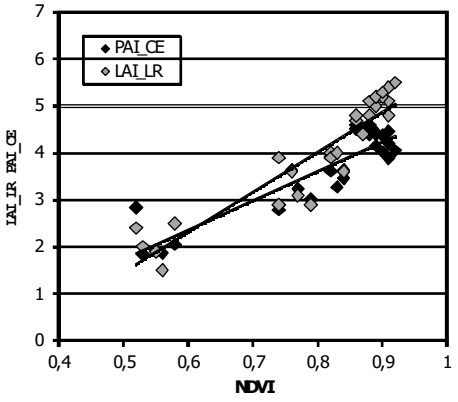

Figure 6. The relationship between LAI_{LR}, PAI_{CE} and NDVI. LAI_{LR} = 8.573NDVI – 2.84, R^2 = 0.85, PAI_{CE} = 6.279NDVI - 1.409, R^2 = 0.82

Assessment of NDVI time series based phenology metrics

All the used methods provided estimate of green-up metric, however, there was a considerable variation (Table 6). The most of the phenex NDVI data fitting methods except DLogistic resulted in the unrealistically early green-up. TIMESAT and *K'* positioned the start of the season, aka green-up, quite close to the *in situ* observed bud swelling phenophase (Table 4) In the beech stands this is probably caused by the earlier growth start of the forest understorey vegetation. The maturity metric was provided by *K'* only and maturity was almost coinciding with the *in situ* observed onset of LU_{100}. The season maximum as calculated by phenex varied in a great extent depending on data fitting method. The earliest estimate of the season maximum was on LU_{100} and the latest estimated DOY was in the middle of FLU. The senescence metric seemed to have different interpretation in *K'* method and in phenex as the phenex estimate of senescence occurred later then dormancy given by *K'* which, on the other hand, corresponded well with the end of season given by TIMESAT (Table phenometrics). Only DLogistic and SavGol data fitting methods in phenex produced realistic values of senescence (interpreted as the end of the season) in some stands at the selected threshold. We also run phenex with local threshold set to 0.2 (data not shown here) which produced later DOY of green-up and earlier DOY for senescence estimates but there was still a considerable variation among the data fitting methods.

Discussion and Conclusions

Satellite remote sensing provides a unique opportunity to monitor vegetation phenology over large areas. For the correct interpretation of the remote sensing data their relationships with the *in situ* observed variables must be well known. The Leaf area index is one of the main driving variables of vegetation reflectance and also an indicator of phenology. We used two different methods, LinearRatio and subjective pixel classification, to estimate the canopy transmittance of

Table 6. The phenology metrics derived from NDVI data with curvature (K') method, phenoPhase method in the Phenex package and module and the TIMESAT software method TSM_printseasons. Different data fitting methods were tested. The phenology metrics, such as green-up, maturity, maximum NDVI, senescence and dormancy, are denoted here with the first three characters of each metric name. The description of phenex and TIMESAT data fitting methods can be found in the software manuals. In phenex and TIMESAT the local (i.e. relative) threshold equal to 0.1 was used to identify the start and the end of the season

Stand	Phenology metrics												
		phenex									Curvature	TIMESAT	
	Metric	LinIP	Spline	DSig	DSigC	DLogistic	Gauss	Growth	FFT	SavGol	*K'*	Logistic	SavGol
509	gre	34	34	17	89	101	57	25	89	94	100	97	100
	mat	-	-	-	-	-	-	-	-	-	124	-	-
	max	139	139	211	149	170	204	201	238	143	-	-	-
	sen	364	364	364	364	364	349	364	330	363	269	-	-
	dor	-	-	-	-	-	-	-	-	-	316	315.1	321
514	gre	97	97	17	95	103	60	26	84	95	101	96.4	101
	mat	-	-	-	-	-	-	-	-	-	124	-	-
	max	146	146	210	156	167	202	201	239	145	-	-	-
	sen	364	364	364	364	333	343	364	329	350	269	-	-
	dor	-	-	-	-	-	-	-	-	-	315	315.9	317
531	gre	57	57	17	89	105	61	26	92	78	103	97	103
	mat	-	-	-	-	-	-	-	-	-	124	-	-
	max	139	139	208	149	161	200	200	158	151	-	-	-
	sen	356	356	363	364	322	339	364	329	341	266	-	-
	dor	-	-	-	-	-	-	-	-	-	316	315.7	320
541	gre	45	45	17	87	104	64	26	9	65	105	95.2	103
	mat	-	-	-	-	-	-	-	-	-	122	-	-
	max	146	146	209	156	161	199	204	173	150	-	-	-
	sen	333	333	354	317	315	334	354	329	319	270	-	-
	dor	-	-	-	-	-	-	-	-	-	315	315	308.6
619	gre	70	70	17	89	96	60	25	37	78	97	99.4	96.4
	mat	-	-	-	-	-	-	-	-	-	125	-	-
	max	146	146	210	156	179	200	205	174	157	-	-	-
	sen	326	326	355	320	316	338	354	324	317	274	-	-
	dor	-	-	-	-	-	-	-	-	-	316	313.4	307.

mature beech forests from hemispherical images over the vegetation period. The transmittance based LAI_{LR} and PAI_{CE} were regressed to NDVI from satellite-borne MODIS images.

The NDVI values during the growing season were analysed according to tree canopy foliage phenology. The onset of phenological phases in a forest is usually identified using the phenological metrics that are based on the inflection points (Fisher and Mustard 2007) or the maximal rate of change in the curvature of the smoothing functions (Zhang et al. 2003, Ahl et al. 2006, Ganguly et al. 2010). In this study, however, we were interested in specific NDVI values in relation to the observed phenophases similar to Soudani et al. (2012), who identified the minimum value of NDVI in the beech forests in France at the date of budburst and the maximum NDVI at the day corresponding to the end of leaves expansion. In the beech stands of this study, the phenophase budburst occurred later than the minimum NDVI. The NDVI increase during the spring was evoked by the strategy of the phenological escape of the understory vegetation and undergrowth (Brandýsová and Bucha 2012). The phenological phases of the beech forest understory begin before the phenophases of canopy trees: a strategic approach to utilize the temporary favourable microclimate and light conditions in forests. This indicates that forests of the same tree species growing on the same continent do not have to reach the same phenophase in relation to NDVI. This depends on climate conditions and forest structures. However, after the budburst the relationship between NDVI and the phenophases of our stands was similar to Soudani et al. (2012) since NDVI started to slightly decrease already after the maximal NDVI and a steep decrease was observed in the early autumn after beginning of leaf yellowing.

The MODIS NDVI followed the phenological phases of foliage during the growth season and indicated a strong linear relationship with LAI_{LR} and PAI_{CE}. For example, Wang et al. (2005) detected strong linear relationships between LAI_{LR} and NDVI only during the periods of leaf production and leaf senescence. Wang et al. (2005) stated that the relationship was poor during the period of maximum LAI_{LR} apparently due to the saturation of NDVI at the high values of LAI_{LR}. One of the most interesting findings in our study was that the relationship between NDVI and LinearRatio-based LAI_{LR} did not saturate at the high values of LAI_{LR}. Many authors (Lüdeke et al. 1991, Toby and Ripley 1997, Wang et al. 2005) have asserted that the NDVI of a pixel with the complete forest cover does not increase after LAI_{LR}

reaches the value over 2(3). Our results revealed, that NDVI of beech stands was increasing until LAI_{LR} reached the maximal area, and NDVI started to decrease already in August with decreasing of LAI_{LR}.

The coefficients of determination calculated in our study were 0.85 between LAI_{LR} and NDVI, and 0.82 between PAI_{CE} and NDVI. However, the overestimation of canopy transmittance and consequent underestimation of the area covered by forest canopy at high PAI_{CE} values in subjective classification of hemispherical image indicated, that LinearRatio based methods should be preferred for canopy transmittance measurements. These phenomena were clearly visible in LAI_{LR} to PAI_{CE} regression and their relationship with NDVI. Many of the existing studies suggested various shapes of relationships between LAI and NDVI. Comparing to other linear relationships, Wang et al. (2005) found that the LAI-NDVI coefficients of determination varied from 0.39 to 0.46 for different sources of NDVI. On the other hand, Potithep et al. (2010) discovered very strong linear LAI-NDVI and LAI-EVI relationships with R^2 = 0.89 and 0.94, respectively. Other studies revealed the NDVI-LAI coefficient of determination equal to 0.19 for forest vegetation type (Colombo et al. 2003), and 0.35, 0.75, and 0.86 for slash pine in Florida in February, September and March, respectively (Curran et al. 1992).

The estimation of canopy leaf area index is prone to different errors and shortcomings in the methods. The methods that are based on the subjective thresholding or pixel classification of hemispherical images to estimate LAI assume that sky radiance is constant over the view of zenith and azimuth angles and that there is no vignetting of the signal. These assumptions are seldom fulfilled. There are usually random fluctuations and systematic changes in sky radiance under both overcast and near sunset or sunrise conditions and the hemispherical lenses or converters on digital cameras have significant vignetting (Lang et al. 2010). Although LinearRatio method of canopy transmittance estimation was more sensitive to the image exposure errors and occasional direct illumination of hemispherical images, the final outcome was better and more realistically related to the actual phenological events.

While the seasonal course of LAI_{LR} showed a very good agreement with the occurring phenological phases, PAI_{CE} values did not, since the PAI_{CE} seasonal course differed from the phenological situation especially in the transition period from spring to summer. These findings were similar to the results of Pavlendová et al. (2009), who derived the seasonal course of effective LAI (LAI_e) for stand 541 in the 2009. Pavlendová et al. (2009) analysed hemispherical photographs in GLA software using subjective tresholding and found the same drop of LAI_e in spring as we revealed for PAI_{CE}. However, such an early decrease in the canopy indices based on the subjective thresholding cannot be explained with any of our field observations of the phenological situation after the end of leaf unfolding. We conclude that the operator's subjective decision distorts the estimates of structural information from hemispherical images and such methods are not suited for phenological studies of forest stands.

The decrease of PAI_{CE} after the phenological phase LU_{100} can be sometimes realistic due to the possible summer drought or biotic agents (insects *etc*.). However, none of such events were recorded in the test sites during our study. It is necessary to note that the development of leaves does not finish with the phenophase of leaf unfolding. After LU_{100}, leaves continue increasing their area, and their width, and change their colour until the phenophase of full leaf unfolding (SHMU 1984), and this is the reason why LAI_{LR} should not decrease. In our test stands it took up to one month to reach the phenophase FLU_{100}. During this period the NDVI values of test forests derived from MODIS images continued to increase, which was in correspondence to the results from Brandýsová and Bucha (2012), who used spectroradiometer LI-1800 with integration sphere 1800-12 and revealed increasing NDVI of beech leaves from DOY 123 with average NDVI 0.71 (s_x = 0.023) to DOY 159 with average NDVI equal to 0.79 (s_x = 0.015).

In our test forests, the leaf area index and NDVI started to decrease after DOY 170 (FLU_{100}). García-Plazaola and Becerril (2001) examined the pigments in Mediterranean beech leaves and found that the pigment content decreased progressively during the summer in sunlit leaves (leaves exposed to the sun) and remained stable in shaded leaves (leaves underneath the sunlit leaves). García-Plazaola and Becerril (2001) discovered that from July to September, there was no chlorophyll biosynthesis, hence, photodegradation of chlorophyll was not compensated by new production. The natural leaf senescence occurred first in sunlit leaves, and during the senescence leaf chlorophyll was completely degraded (García-Plazaola and Becerril 2001). This agrees with the slight decrease of NDVI from July to September followed by a faster decrease until the winter season in our test stands.

When deriving LAI from hemispherical images, an effect of terrain slope must be taken into account. Espańa et al. (2008) discovered potential strong underestimation of LAI higher than 2 on slopes steeper than 25°. Since the forest stands in this study were located on slopes less than 25°, the only correction we performed was masking out the slope terrain. Simi-

larly, vegetation indices can also be affected by the terrain topography. However, the indices which can be expressed as a function of the ratio vegetation index (RVI) like NDVI can almost completely reduce the direct effect of topography (Matsushita et al. 2007). Although EVI is considered as a better indicator of plant phenology than NDVI (Heute et al. 2002), it cannot be expressed as a function of RVI because of the soil adjustment factor (Matsushita et al. 2007). Due to the sloping terrain of our test stands, NDVI seems to be a better vegetation index than EVI.

Data smoothing and filtering is usually the first step required for estimation of phenology metrics from NDVI data series. The NDVI series in our test were carefully cleaned first by using the quality control data of the MODIS daily surface reflectance product and additional smoothing was not applied. Thus, the estimated phenology metrics depended mainly on the selection of data fitting model and applied settings. We can confirm conclusions of Hird and McDermid (2009), who found double logistic function superior over other data fitting techniques for NDVI phenology series. However, after selecting the best model there is the final step – the actual value of a metric has to be calculated according to some rule. In phenex and TIMESAT software the rule is based on a threshold for the NDVI to determine start and end of season. Estimation of the threshold is difficult and almost subjective without having some previous *in situ* observations for the ecosystem under study. The same threshold can produce different values for the same phenology metric in different programs. On the other hand, the model curvature based estimation of phenology metrics, which is proposed by Zhang et al. (2003), did not require any additional settings and the results were well described by *in situ* observations.

European beech is one of the most frequent tree species covering the large area of Europe (Magri 2008). Monitoring of its reactions to the changing climate conditions could support silvicultural decisions in future. In this study we investigated the options to monitor vegetation phenology of mature beech stands using daily MODIS NDVI. A strong linear relationship between NDVI and LAI of beech stands was observed and the relationship was not saturated at high LAI values in summer. The analysis of *in situ* observed phenological phases and leaf area indices based on digital hemispherical images confirmed the applicability of MODIS NDVI for phenological monitoring. Since off-the-shelf cameras are not originally intended for measurements but for photography, it is important to choose appropriate settings for the cameras. However, the estimation of canopy indices can be performed in existing software like CanEye, which can directly use canopy transmittance data. For further phenological studies that plan to use hemispherical images we recommend to store the images in raw data format as this enables to use the LinearRatio based methods for the canopy transmittance calculation. For phenology observation at flux towers such raw data from downward looking digital cameras equipped with regular lenses are already successfully used (Ahrends et al. 2008, Richardson et al. 2009).

Acknowledgements

This study was funded by VEGA MŠ SR: nos. 1/0281/11 and 1/0257/11, APVV-0423-10 and APVV-0303-11, and Estonian Science Foundation Grant No. 8290. We thank Tiit Nilson for the comments on the early version of the manuscript. The manuscript was significantly improved following the recommendations from two anonymous reviewers. The authors thank Lars Eklundh for help on TIMESAT linux version installation.

References

Ahl, D. E., Gower, S. T., Burrows, S. N., Shabanov, N. V., Myneni, R. B. and Knyazikhin, Y. 2006. Monitoring spring canopy phenology of a deciduous broadleaf forest using MODIS. *Remote Sensing of Environment* 104: 88–95.

Ahrends, H. E., Brügger, R., Stöckli, R., Schenk, J., Michna, P., Jeanneret, F., Wanner, H. and Eugster, W. 2008. Quantitative phenological observations of a mixed beech forest in northern Switzerland with digital photography. *Journal Geophysical Research* 113: G04004, doi:10.1029/2007JG000650.

Badeck, F.-W., Bondeau, A., Böttcher, K., Doktor, D., Lucht, W., Schaber, J. and Sitch, S. 2004. Responses of spring phenology to climate change. *New Phytologist* 162: 295–309.

Baret, F. and Weiss, M. 2010. CAN-EYE V6. User manual, URL: *https://www4.paca.inra.fr/can-eye/Documentation-Publications/Documentation* (last date accessed: February the 1., 2013).

Bartzokas, A., Darula, S., Kambedzidis, H.D, and Kittler, R. 2003. Sky luminance distribution in Central Europe and Maditerranean area during winter period. *Journal of Atmospheric and Solar-Terrestrial Physics* 64: 113–119.

Beck, P. S. A., Atzberger, C., Høgda, K. A., Johansen, B. and Skidmore, A. K. 2006. Improved monitoring of vegetation dynamics at very high latitudes: A new method using MODIS NDVI. *Remote Sensing of Environment* 100: 321–334.

Brandýsová, V. and Bucha, T. 2012. Vplyv prķzemnej vegetţcie a podrastu na priebeh fenologickej krivky bukovžch porastov odvodenej z šdajov MODIS [Effect of understory vegetation and undergrowth on course of phenological curve of beech forests derived from MODIS]. *Lesnícky Časopis – Forestry Journal* 58(4): 231–242 (in Slovak with English summary).

Bucha, T. 1999. Classification of tree species composition in Slovakia from satellite images as a part of monitoring

forest ecosystems biodiversity. *Acta Instituti Forestalis Zvolen* 9: 65–84.

Cescatti, A. 2007. Indirect estimates of canopy gap fraction based on the linear conversion of hemispherical photographs: methodology and comparison with standard thresholding techniques. *Agricultural and Forest Meteorology* 143: 1–12.

Chazdon, R. L. and Field, C. B. 1987. Photographic estimation of photosynthetically active radiation: evaluation of a computerized technique. *Oecologia* 73: 525–532.

Chmielewski, F. M. and Rötzer, T. 2001. Response of tree phenology to climate change across Europe. *Agricultural and Forest Meteorology* 108: 101–112.

Coffin, D. 2011. Decoding raw digital photos in Linux. URL: http://www.cybercom.net/~dcoffin/dcraw/ (date accessed: September the 13., 2013).

Colombo, R., Bellingeri, D., Fasolini, D. and Marino, C. M. 2003. Retrieval of leaf area index in different vegetation types using high resolution satellite data. *Remote Sensing of Environment* 86 (1): 120–131.

Curran, P. J., Dungan, J. F. and Gholz, H. L. 1992. Seasonal LAI in slash pine estimated with Landsat TM. *Remote Sensing of Environment* 39(1): 3–13.

Čufar, K., Luis, M. D., Saz, M. A., Črepinšek, Z. and Kajfež-Bogataj, L. 2012. Temporal shifts in leaf phenology of beech (*Fagus sylvatica*) depend on elevation. *Trees* 26: 1091–1100.

Eklundh, L. and Jönsson, P. 2011. TIMESAT 3.1 Software Manual, Lund University, Sweden.

Espańa, M. L., Baret, F. and Weiss, M. 2008. Slope correction for LAI estimation from gap fraction measurements. *Agricultural and Forest Meteorology* 148: 1553–1562.

Fisher, J. I. and Mustard, J. F. 2007. Cross-scalar satellite phenology from ground, Landsat and MODIS data. *Remote Sensing of Environment* 109: 261–273.

Ganguly, S., Friedl, M. A., Tan, B., Zhang, X. and Verma, M. 2010. Land surface phenology from MODIS: Characterization of the Collection 5 global cover Dynamics product. *Remote Sensing of Environment* 114: 1805–1816.

García-Plazaola, J. I. and Becerril, J. M. 2001. Seasonal changes in photosynthetic pigments and antioxidants in beech (*Fagus sylvatica*) in a Mediterranean climate: implications for tree decline diagnosis. *Australian Journal of Plant Physiology* 28(3): 225–232.

Guyon, D., Guillot, M., Vitasse, Y., Cardot, H., Hagolle, O., Delzon, S. and Wigneron, J. P. 2011. Monitoring elevation variations in leaf phenology of deciduous broadleaf forests from SPOT/VEGETATION time-series. *Remote Sensing of Environment* 115: 615–627.

Heinsch, F. A., Matt, R., Votava, P., Kang, S., Milesi, C., Zhao, M., Glassy, J., Jolly, W. M., Loehman, R., Bowker, C. F., Kimball, J. S., Nemani, R. R. and Running, S. W. 2003. User's Guide. GPP and NPP (MOD17A2/A3) Products. NASA MODIS Land Algorithm. Version 2.0, December 2, 2003. URL: http://www.ntsg.umt.edu/sites/ntsg.umt.edu/files/modis/MOD17UsersGuide.pdf (last date accessed: September the 30., 2013).

Heute, A., Didan, K., Miura, T., Rodriguez, E. P., Gao, X. and Ferreira, L. G. 2002. Overview of the radiometric and biophysical performance of the MODIS vegetation indices. *Remote Sensing of Environment* 83: 195–213.

Hird, J. and McDermid, G. J. 2009. Noise reduction of NDVI time series: An empirical comparison of selected techniques. *Remote Sensing of Environment* 113(1): 248"258.

Jennings, S. B., Brown, N. D. and Sheil, D. 1999. Assessing forest canopies and understorey illumination: canopy closure, canopy cover and other measures. *Forestry* 72: 59–73.

Jeong, S.-J., Ho, CH.-H., Gim, H.-J. and Brown, M. E. 2011: Phenology shifts at start vs. end of growing season in temperate vegetation over the Northern Hemisphere for the period 1982–2008. *Global Change Biology* 17: 2385–2399.

Jonckheere, I., Fleck, S., Nackaerts, K., Muys, B., Coppin, P., Weiss M. and Baret, F. 2004. Review of methods for in situ leaf area index determination: Part I. Theories, sensors and hemispherical photography. *Agricultural and forest meteorology* 121: 19–35.

Jonckheere, I., Nackaerts, K., Muys, B. and Coppin, P. 2005. Assessment of automatic gap fraction estimation of forests from digital hemispherical photography. *Agricultural and Forest management* 132: 96–114.

Jönsson, P. and Eklundh, L. 2002. Seasonality extraction and noise removal by function fitting to time-series of satellite sensor data. *IEEE Transactions of Geoscience and Remote Sensing* 40(8): 1824"1832.

Jönsson, P. and Eklundh, L. 2004. Timesat - a program for analyzing time-series of satellite sensor data. *Computers and Geosciences* 30: 833"845.

Jönsson, A. M., Hellström, M., Bärring, L. and Jönsson, P. 2010. Annual changes in MODIS vegetation indices of Swedish coniferous forests in relation to snow dynamics and tree phenology. *Remote Sensing of Environment* 114: 2719–2730.

Justice, C. O., Townshend, J. R. G., Vermote, E. F., Masuoka, E., Wolfe, R. E., Saleous, N., Roy, D. P. and Morisette, J. T. 2002: An overview of MODIS land data processing and product status. *Remote Sensing of Environment* 83: 3–15.

Kodar, A., Kutsar, R., Lang, M., Lükk, T. and Nilson, T. 2008. Leaf Area Indices of Forest Canopies from Optical Measurement. *Baltic forestry* 14: 185–194.

Kuusk, A. and Nilson, T. 2000. A directional multispectral forest reflectance model. *Remote Sensing of Environment* 72: 244–252.

Lang, M., Kuusk, A., Mõttus, M., Rautiainen, M. and Nilson, T. 2010. Canopy gap fraction estimation from digital hemispherical images using sky radiance models and a linear conversion method. *Agricultural and Forest Meteorology* 150: 20–29.

Lange, M. and Doktor, D. 2013. Phenex version 1.0.3 - auxiliary functions for phenological data analysis. A package for R-statistical software. Available from CRAN repositories for R.

Liang, L., Schwartz, M. D. and Fei, S. 2011. Validating satellite phenology through intensive ground observation and landscape scaling in a mixed seasonal forest. *Remote Sensing of Environment* 115: 143"157.

Liang, S. 2004. Quantitative remote sensing of land surfaces. John Wiley & Sons, Inc. Hoboken, New Yersey. 534 pp.

Lüdeke, M., Janecek, A. and Kohlmaier, G. H. 1991. Modelling the seasonal CO_2 uptake by land vegetation using the global vegetation index. *Tellus B* 43: 188–196.

Magri, D. 2008: Patterns of post-glacial spread and the extent of glacial refugia of European beech (*Fagus sylvatica*). *Journal of Biogeography* 35: 450–463.

Matsushita, B., Yang, W., Chen, J., Onda, Y. and Qiu, G. 2007. Sensitivity of the Enhanced Vegetation Index (EVI) and Normalized Difference Vegetation Index (NDVI) to Topographic Effects: A Case Study in High-Density Cypress Forest. *Sensors* 7: 2636–2651.

Menzel, A. 2000. Trends in phenological phases in Europe between 1951 and 1996. *International Journal of Biometeorology* 44: 76–81.

Menzel, A. 2002. Phenology: its importance to the global change community. *Climatic Change* 54: 379–385.

Narasimhan, R. and Stow, D. 2010. Daily MODIS products for analyzing early season vegetation dynamics across the North Slope of Alaska. *Remote Sensing of Environment* 114: 1251–1262.

Nilson, T. 1999. Inversion of gap frequency data in forest stands. *Agricultural and Forest Meteorology* 98–99: 437–448.

Nilson, T. and Kuusk, A. 2004. Improved algorithm for estimating canopy indices from gap fraction data in forest canopies. *Agricultural and Forest Meteorology* 124 (3–4): 157–169.

Pavlendová, H., Barka, I., Bucha, T. and Priwitzer, T. 2009. Odvodenie indexu listovej plochy z Modisu [Derivation of laef area index from MODIS]. In: Bucha, T., Pavlendová, H. (Editors), Dial'kový prieskum Zeme – Lesy v meniacich sa prírodných podmienkach. Vedecký seminar, Zvolen, NLC - LVÚ, p. 65–80 (in Slovak with English abstract).

Potithep, S., Nasahara, N.K., Muraoka, H., Nagai, S. and Suzuky, R. 2010. What is the actual relationship between LAI and VI in a deciduous broadleaf forest? *International Archives of the Photogrammetry, Remote Sensing and Spatial Information Science* 38 (8): 609"614.

R Core Team 2012. R: A language and environment for statistical computing. R Foundation for Statistical Computing, Vienna, Austria. ISBN 3-900051-07-0, URL http://www.R-project.org/.

Regent Instruments Inc. © 2013. WinSCANOPY. URL: *http://www.regent.qc.ca/assets/winscanopy_about.html* (last date accessed: October the 17., 2013).

Richardson, A. D., Braswell, B. H., Hollinger, D. Y., Jenkins, J. P. and Ollinger, S. V. 2009. Near-surface remote sensing of spatial and temporal variation in canopy phenology. *Ecological Applications* 19: 1417"1428. http://dx.doi.org/10.1890/08-2022.1.

SHMU 1984. Nįvod na fenologické pozorovanie lesnżch rastlķn [Instructions for phenological monitoring of forest plants]. Bratislava, Slovakia, 25 pp. (in Slovak).

Soudani, K., Hmimina, G., Delpierre, N., Pontailler, J.-Y., Aubinet, M., Bonal, D., Caquet, B., Grandcourt, A., Burban, B., Flechard, C., Guyon, D., Granier, A., Gross, P., Heinesh, B. Longdoz, B., Loustau, D., Moureaux, C., Ourcival, J.-M., Rambal, S., Saint André, L. and Dufrêne, E. 2012. Ground-based Network of NDVI measurements for tracking temporal dynamics of canopy structure and vegetation phenology in different biomes. *Remote Sensing of Environment* 123: 234–245.

Soudani, K., Maire, G., Dufrêne, E., François, CH., Delpierre, N., Ulrich, E. and Cecchini, S. 2008. Evaluation of the onset of green-up in temperate deciduous broadleaf forests derived from Moderate Resolution Imaging Spectroradiometer (MODIS) data. *Remote Sensing of Environment* 112: 2643–2655.

Sparks, T. H. and Carey, P. D. 1995. The responses of species to climate over two centuries: an analysis of the Marsham phenological record, 17361947. *Ecology* 83: 321–329.

Ter Steege, H. 1997. WINPHOT. A Windows 3.1 programme to analyse vegetation indices, light and light quality from hemisperical photographs. Tropenbos-Guyana Reports 97-3, Tropenbos-Guyana Programme, Georgetown, Guyana.

Toby, N. C. and Ripley D., A. 1997. On the Relation between NDVI, Fractional Vegetation Cover, and Leaf Area Index. *Remote Sensing of Environment* 62: 241–252.

Tucker, C. J. 1979. Red and photographic infrared linear combinations for monitoring vegetation. *Remote Sensing of Environment* 8: 127 – 150.

Vermote E. F., Kotchenova, S. Y. and Ray, J. P. 2011. MODIS Surface Reflectance User's Guide. URL: *http://modis-sr.ltdri.org/products/MOD09_UserGuide_v1_3.pdf* (last date accessed: September the 27., 2013).

Walter, J.-M. 2009. CIMES-FISHEYE. Hemispherical Photography of Forest Canopies. A Package of Programs for the Determination of Canopy Geometry and Solar Radiation Regimes through Hemispherical Photographs. Université de Strasbourg, France URL: *http://jmnw.free.fr/* (last date accessed: February the 1., 2013).

Wang, G., Adiku, S., Tenhunen, J. and Granier, A. 2005. On the relationship of NDVI with leaf area index in a deciduous forest site. *Remote Sensing of Environment* 94: 244"255.

Watson, D. J. 1947. Comparative physiological studies in growth of field crops. 1. Variation in net assimilation rate and leaf area between years. *Annals of Botany* 11: 41–76.

Weiss, M., Baret, F., Smith, G. J., Jonckheere, I., Coppin, P. 2004. Review of methods for in situ leaf area index (LAI) determination: Part II. Estimation of LAI, errors and sampling. Agricultural and Forest Meteorology, 121: 37–53

Wolfe, R. E., Nishihama, M., Fleig, A. J., Kuyper, J. A., Roy, D. P., Storey, J. C. and Pat, F. S. 2002. Achieving sub-pixel geolocation accuracy in support of MODIS land science. *Remote Sensing of Environment* 83: 31–49.

Zhang, X., Friedl, M. A., Schaaf, C. B., Strahler, A. H., Hodges, J. C. F., Gao, F., Reed, B. C. and Heute, A. 2003. Monitoring vegetation phenology using MODIS. *Remote Sensing of Environment* 84: 471–475.

Received 07 February 2013
Accepted 21 October 2014

СЕЗОННЫЕ ИЗМЕНЕНИЯ ИНДЕКСОВ NDVI, LAI И PAI ОТНОСИТЕЛЬНО ФЕНОЛОГИЧЕСКИХ ФАЗ БУКОВЫХ ЛЕСОВ

В. Лукасова, М. Ланг и Я. Шкваренина

Резюме

Наступление фенологических фаз, таких как раскрытие почки, развитие листа, цветение, плодоношение и старение листа, вызвано генетически зависимой внутренней периодичностью растительности и в значительной степени зависит от климатических условий. Поэтому сроки наступления фенологических фаз считаются хорошим индикатором последствий изменения климата. Фенологические фазы экосистем можно наблюдать со спутников используя изменения в спектральной яркости, которая главным образом обусловлена оптическими свойствами, расположением и площадью листа.

В этом исследовании мы использовали вегетационный индекс NDVI (Normalized Difference Vegetation Index) в качестве индикатора сезонной динамики буковых лесов (*Fagus sylvatica* L.) на 5 пробных площадях в Словакии. Мы проанализировали фенологические фазы на каждой пробной площади в течение одного вегетационного периода, используя три разных подхода: I) фенологические наблюдения на месте, II) цифровые полусферические изображения, снятые, чтобы охарактеризовать изменения листового индекса LAI (Leaf Area Index) и индекса PAI (Plant Area Index), III) вегетационный индекс NDVI, вычисленный на основе космических данных радиометра MODIS. Оценки индексов LAI и PAI напрямую зависят от точности оценивания доли просветов в пологе (коэффициент прозрачности), полученных с полусферических снимков. Таким образом, мы проверили классификацию пикселей, основанную на субъективном решении оператора, и недавно предложенном линейном преобразовании данных необработанного снимка (LinearRatio), которое, как было выявлено, приводит к сопоставимым результатам с наиболее часто используемыми анализаторами полога растительности.

Результаты показали, что значения NDVI чутко реагировали на изменения вегетационных фенологических фаз. Наиболее быстрое увеличение NDVI было зафиксировано во время фазы разворачивающегося листа. После достижения максимума значения, NDVI на всех пробных площадях начали медленно снижаться в течение летнего периода. За этим последовало быстрое снижение значений осенью во время фазы старения листа. Основные изменения индекса NDVI хорошо объясняются изменениями индекса LAI, однако, влияние метода оценки LAI было значительным. Коэффициент прозрачности полога, вычисленный с субъективно классифицированных полусферических изображений, начал увеличиваться уже в мае, тогда как доля просветов в пологе, вычисленная по методу LinearRatio, продолжала уменьшаться до конца июля, что находится в соответствии с данными натурных наблюдений. Оценки LAI при использовании метода LinearRatio для вычисления доли просветов в пологе не зафиксировали насыщенности связи между NDVI при высоких значениях LAI (LAI > 3), как на это указывают многие авторы. Согласно нашим результатам, MODIS NDVI может использоваться для наблюдения фенологических фаз зрелых буковых лесов. Для вычисления коэффициента прозрачности, который требуется для оценки листового индекса LAI с полусферических изображений, мы рекомендуем использовать методики, базирующиеся на LinearRatio.

Ключевые слова: бук, NDVI, LAI, PAI, фенологические фазы